



Universiteit  
Leiden  
The Netherlands

## DNA repair and gene targeting in plant end-joining mutants

Jia, Q.

### Citation

Jia, Q. (2011, April 21). *DNA repair and gene targeting in plant end-joining mutants*. Retrieved from <https://hdl.handle.net/1887/17582>

Version: Corrected Publisher's Version

License: [Licence agreement concerning inclusion of doctoral thesis in the Institutional Repository of the University of Leiden](#)

Downloaded from: <https://hdl.handle.net/1887/17582>

**Note:** To cite this publication please use the final published version (if applicable).

## **Chapter 4**

AtKu80 and AtParp are involved  
in distinct NHEJ pathways

Qi Jia, Amke den Dulk-Ras, B. Sylvia de Pater and  
Paul J.J. Hooykaas

## Abstract

Besides the Ku-dependent classical non-homologous end joining (C-NHEJ) pathway, an alternative NHEJ pathway has been identified in mammalian systems, which is often called the back-up NHEJ (B-NHEJ) pathway. The single-strand break repair factor poly (ADP-ribose) polymerase (Parp) was found to be involved in B-NHEJ in mammalian cells. In B-NHEJ, micro-homology is often used for repair. In order to investigate alternative pathways for NHEJ in Arabidopsis, the *Atparp1parp2ku80* (*Atp1p2k80*) mutant was obtained and functionally characterized along with the *Atku80* and *Atparp1parp2* (*Atp1p2*) mutants. Due to the absence of both the C-NHEJ factor AtKu80 and the putative B-NHEJ factors AtParp1 and AtParp2, the *Atp1p2k80* mutant was hypersensitive to DNA damage agents resulting in more DNA damage, but it still had the ability to repair DNA damage as measured in comet assays. The absence of AtParp proteins restored end joining in the background of AtKu80-deficient plants, suggesting the presence of another alternative NHEJ pathway, which is suppressed by AtKu and AtParp proteins under normal conditions. End joining assays with different linear DNA substrates with different ends in cell-free leaf protein extracts showed that AtKu played a role in DNA end protection and AtParp proteins were involved in micro-homology mediated end joining (MMEJ). The *Atp1p2k80* mutant showed a reduced T-DNA integration efficiency after floral dip transformation. The gene targeting frequency of the triple mutant was not significantly different from that of the wild-type.

## Introduction

For living organisms, DNA double strand breaks (DSBs) are one of the most harmful lesions that can promote mutation and induce cell death. There are two primary pathways to repair DNA DSBs: non-homologous end joining (NHEJ) and homologous recombination (HR). NHEJ is a DNA repair pathway, which rejoins the DNA ends directly and does not depend on homology. HR utilizes a homologous stretch of DNA as a template to align and join the DNA ends. HR is the major pathway used in lower eukaryotes like yeast, whereas NHEJ is the prevailing pathway in higher eukaryotes, such as mammals and plants. DNA transformation also depends on integration of the newly transformed genes by HR or NHEJ (1-3). When NHEJ is blocked in yeast, integration occurs exclusively by HR (2;3). This could open a possibility for increasing the frequency of gene targeting (GT) in plants and mammals. GT is a useful technique for the modification of endogenous genes using HR, but unfortunately occurs with a very low frequency in higher eukaryotes.

Distinct NHEJ pathways have been identified in mammals. One is the classical NHEJ (C-NHEJ) pathway, which is dependent on Ku70/Ku80 and DNA-PKcs. DNA ligase IV (Lig4), XRCC4 and XLF/Cernunnos are also utilized as central components in C-NHEJ.

In the absence of C-NHEJ core factors, back-up NHEJ (B-NHEJ) pathways were identified (4). Some proteins were shown to be involved in B-NHEJ, such as Parp1, Parp2, DNA ligase III (Lig3) and XRCC1 (5;6). In the absence of C-NHEJ, micro-homologous sequences (5-25 bps) flanking the break are more frequently used to join the DNA ends, resulting in deletions. This error-prone pathway has been called micro-homology mediated end joining (MMEJ). It seemed that MMEJ is the predominant pathway among the B-NHEJ pathways. Most components involved in MMEJ are still elusive.

In plants, homologs for most mammalian C-NHEJ factors have been identified, suggesting a similar NHEJ mechanism. However, the existence of B-NHEJ pathways and the proteins involved is still unclear. Here we hypothesized that Parp proteins were also involved in B-NHEJ in plants as in mammals. The triple mutant *Atparp1parp2ku80* (*Atp1p2k80*) was obtained and functionally characterized. The sensitivity to DNA damage and the end joining activity were tested for this triple mutant, and T-DNA integration and gene targeting were also analyzed.

## 4

### Material and methods

#### Plant material

The *Atparp1*, *Atparp2* and *Atku80* T-DNA insertion lines were obtained from the GABI-Kat T-DNA collection (GABI-Kat Line 692A05) or the SALK T-DNA collection (SALK\_640400, SALK\_016627), respectively. Information about it is available at <http://signal.salk.edu/cgi-bin/tdnaexpress> (7). The homozygotes of those mutants isolated in our lab (chapter 2 and 3) were crossed and the homozygous *Atparp1parp2* (*Atp1p2*) double mutant and the homozygous *Atparp1parp2ku80* (*Atp1p2k80*) triple mutant were obtained.

#### Assays for sensitivity to bleomycin and methyl methane sulfonate (MMS)

Seeds of wild-type, *Atp1p2*, *Atp1p2k80* and *Atku80* plants were surface-sterilized as described (8) and germinated on solid ½ MS medium (9). Four days after germination, the seedlings were transferred to liquid ½ MS medium without additions or ½ MS medium containing 0.2 µg/ml and 0.4 µg/ml Bleocin<sup>TM</sup> (Calbiochem), 0.007% and 0.01% (v/v) MMS (Sigma). The seedlings were scored after 2 weeks of growth. Fresh weight (compared with controls) was determined by weighing the seedlings in batches of 20 in triplicate, which were treated in 0%, 0.006%, 0.008% and 0.01% (v/v) MMS for 2 weeks.

#### Comet assay

One-week-old seedlings were treated in liquid ½ MS containing 0.01% MMS for 0 h, 2 h and 24 h. Some seedlings with 24 h treatment were recovered in liquid ½ MS for another 24 h. DNA damage was detected by comet assays using the A/N protocol as described in chapter 3. The fraction of DNA in comet tails (%tail-DNA) was used as a measure of DNA damage (10). Measures included 4 independent gel replicas totaling about 100 comets

analyzed per experimental point. The result was represented by the mean value ( $\pm$ standard deviation = S.D.) from four gels, based on the median values of %tail-DNA of 25 individual comets per gel. The student's t-test was used to test for significant difference compared to the wild-type with the same treatment.

### ***In vivo* end joining assay**

Arabidopsis mesophyll protoplasts isolation and protoplasts DNA transformation using the polyethylene glycol (PEG) transformation protocol (11) were described in chapter 2. In each experiment,  $2 \times 10^4$  protoplasts were transformed with 2  $\mu$ g of circular or linear plasmid pART7-HA-GFP(S65T) (Figure 1), which was cleaved with BamHI. Recircularization of

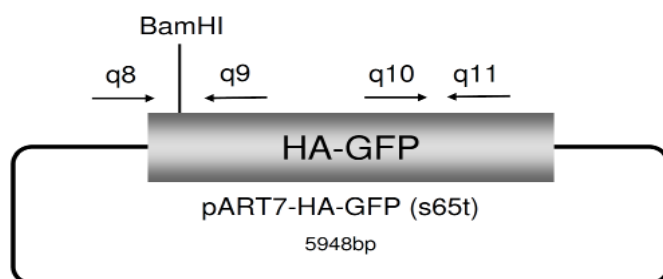


**Figure 1.** Schematic diagram of pART7-HA-GFP.

The primers for Q-PCR are shown by arrows.

**Table 1.** Sequences of primers used for end joining assays.

Name	Sequence
q8	5'-GTGACATCTCCACTGACGTAAG-3'
q9	5'-GATGAACTTCAGGGTCAGCTTG-3'
q10	5'-CAAGCTGACCCTGAAGTTCATC-3'
q11	5'-GTTGTGGCGGATCTTGAAG-3'
q30	5'-GTTTCGGTGATGACGGTG-3'
q31	5'-TGGCACGACAGGTTTCC-3'
q40	5'-GCTGTAGGATGGTAGCTTGGCAC-3'
q41	5'-ATCCTACAGCTGGAATTCGTAATC-3'
q46	5'-TGGAATTCGTAATCATGGTCATAGC-3'
q47	5'-CGTTGGATCCGAATTCGTAATCATGGTCATAGC-3'
q48	5'-CGTTGGTACCGAATTCGTAATCATGGTCATAGC-3'
q49	5'-CGTTGAGCTCGAATTCGTAATCATGGTCATAGC-3'
q50	5'-CGATGGATCCGCTGTAGGATGGTAGCTTG-3'
q51	5'-CGTTGGTACCGCTGTAGGATGGTAGCTTG-3'
q52	5'-CGTTGAGCTCGCTGTAGGATGGTAGCTTG-3'
q53	5'-CGTTGAATTCGCTGTAGGATGGTAGCTTG-3'
PPO-PA	5'-GTGACCGAGGCTAAGGATCGTGT-3'
PPO-1	5'-GCAAGGAGTTGAAACATTAG-3'
PPO-4	5'-CATGAAGTTGTTGACCTCAATC-3'
Sp319	5'-CTATCAAAGAGCACAGACAGC-3'

the linear plasmid in protoplasts was analyzed by Q-PCR with two pairs of primers: q8+q9 and q10+q11 (chapter 2). The sequences of the primers are listed in Table 1. The efficiency of end joining is presented by the ratio of PCR products using q8+q9 primers and q10+q11 primers in comparison with the controls. The value obtained with wild-type protoplasts was set on 1. Q-PCR was performed as three replicates and the assays were performed in triplicate. The PCR products with the primers of q8 and q9 were purified with QIAquick gel extraction kit (Qiagen) and cloned into pJET1.2/blunt Cloning Vector (CloneJET™ PCR Cloning Kit, Fermentas). Individual clones were first digested by BamHI. The clones resistant to digestion by BamHI were sequenced by ServiceXS.

### *In vitro* end joining assay

Protein extracts were obtained from leaves as described in chapter 3. The DNA substrates with different ends were amplified by PCR with different sets of primers. The template for all the PCRs was the 3kb plasmid pUC18P1/4 (chapter 3), which was obtained from Liang (12;13). Phusion™ DNA high-fidelity polymerase (Finnzymes) was used for PCR to generate blunt ends. Sticky ends were generated by digesting the PCR products with different restriction enzymes. The different ends are also listed in Table 2.

**Table 2.** Different ends for end joining assay.

End type			Restriction enzyme	Recognize site	Primers
Sticky ends	Compatible	3'-overhangs	KpnI	GGTAC^C	q48+q51
		5'-overhangs	BamHI	G^GATCC	q47+q50
	Incompatible	3'-overhangs +5'-overhangs	KpnI EcoRI	GGTAC^C G^AATTC	q48+q51
Blunt ends	With micro-homology (10bp)				q40+q41
	Without micro-homology				q40+q46

The linear DNA substrates (300 ng) were incubated with 1 µg protein extract from leaves in 50 mM Tris-HCl (pH7.6), 10mM MgCl<sub>2</sub>, 1mM dithiothreitol, 1 mM ATP and 25% (w/v) polyethylene glycol 2000 at 14°C for 2 hour in a volume of 20 µl. DNA products were purified by electrophoresis through 0.6% agarose gels. A 600-bp fragment containing the end-joined junction was amplified with q30 and q31 primers flanking the junction by PCR, followed by purification and cloning into pJET1.2/blunt Cloning Vector as mentioned above. Individual clones were first digested by corresponding restriction enzymes to check if they were joined precisely or via MMEJ. The clones resistant to the digestion were sequenced by ServiceXS.

### Floral dip transformation and gene targeting

Floral dip transformation was performed according to the procedure described by Clough and Bent (14). The *Agrobacterium* strain AGL1 (pSDM3834) (15) was used for infection. Plasmid pSDM3834 is a pCambia 1200 derivative (hpt selection marker). Seeds were harvested from the dry plants after maturation and plated on solid MA medium (16) without sucrose containing 15 µg/ml hygromycin, 100 µg/ml timentin (to kill *Agrobacterium* cells) and 100 µg/ml nystatin (to prevent growth of fungi). Hygromycin-resistant seedlings were scored 2 weeks after germination and transformation frequency was determined (50 seeds is 1 mg) (17).

In order to test the frequency of gene targeting in the mutants, the same procedure was performed with *Agrobacterium* strain AGL1 (pSDM3900) using the protoporphyrinogen oxidase (PPO) system (18). Plasmid pSDM3900 is a pCambia 3200 derivative (phosphinothricin (ppt) selection marker). About 1 gram seeds were plated on solid MA without sucrose containing 15 µg/ml ppt, 100 µg/ml timentin and 100 µg/ml nystatin to determine the transformation frequency. The rest of the seeds were all sowed on solid MA without sucrose containing 50 µM butafenacil, 100 µg/ml timentin and 100 µg/ml nystatin to identify gene targeting events. The butafenacil-resistant plants were analyzed with PCR to determine if they represent true gene targeting (TGT) events (Figure 2).

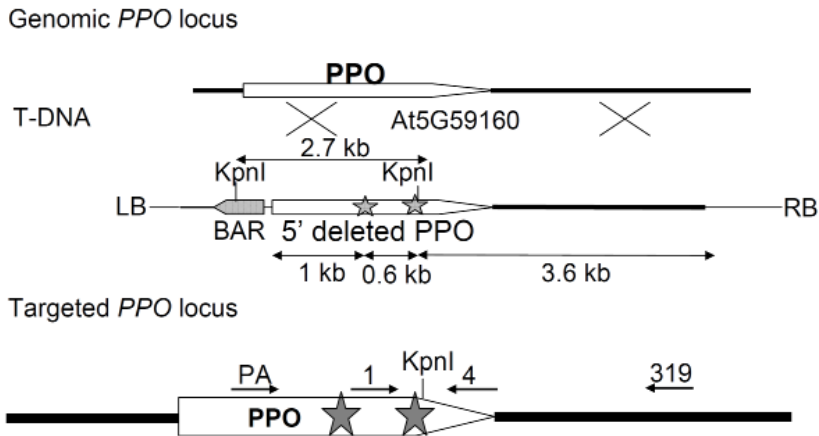


**Figure 2.** The design for the targeted modification of the Arabidopsis *PPO* locus. The white box marked *PPO* represents the *PPO* coding region, and the black lines represents flanking plant genomic DNA. The two mutations conferring butafenacil resistance are indicated as stars. The T-DNA repair construct contains the *BAR* resistance gene linked to the truncated 5'Δ*PPO* (LB for left border and RB for right border). The primers for PCR analysis of the gene targeting events are indicated by arrows.

## Results

### DNA damage response of the *Atku80*, *Atp1p2* and *Atp1p2k80* mutants

In order to study whether the AtParp proteins and the AtKu80 protein function in

different or similar DNA repair pathways, the *Atp1p2k80* triple mutant was obtained and the homozygotes were identified using PCR analysis (chapter 2 and 3). The *Atp1p2k80* mutant had no obvious phenotype under normal growth conditions as compared with the wild-type. When it was treated with genotoxic agents (bleomycin or MMS), it was more sensitive to both agents than the *Atp1p2* and *Atku80* mutants (Figure 3). The radiomimetic chemical bleomycin induces mainly DNA double strand breaks (DSBs) (19), whereas the monofunctional alkylating agent MMS induces mainly DNA single strand breaks (SSBs)

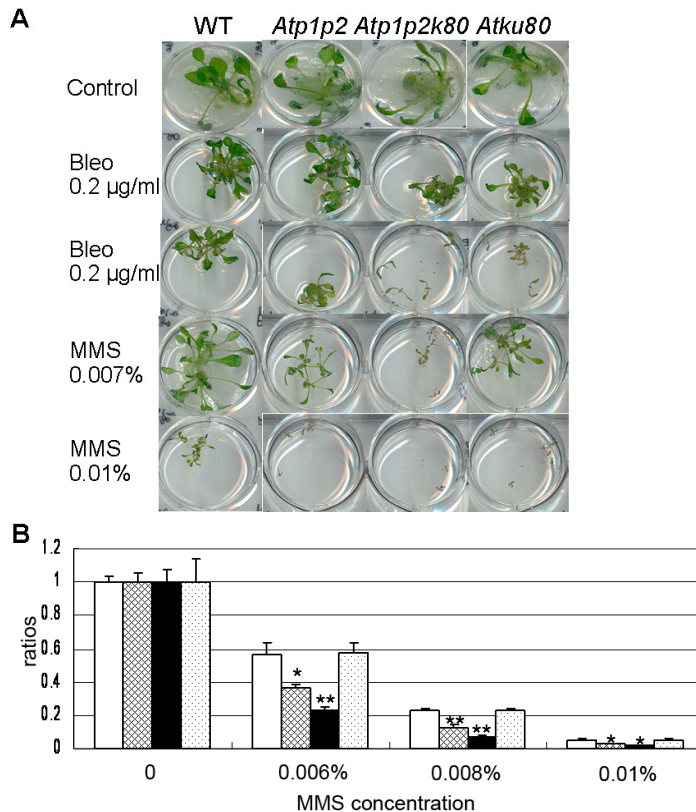


**Figure 3.** Response to DNA-damaging treatments.

(A) Phenotypes of wild-type plants and *Atp1p2*, *Atp1p2k80* and *Atku80* mutants after bleomycin or MMS treatment. Four-day-old seedlings germinated on solid ½ MS were transferred to liquid ½ MS medium (control) or ½ MS medium containing different concentrations of bleomycin (Bleo) or MMS and were scored 2 weeks after germination.

(B) Fresh weight of 2-week-old wild-type plants, *Atp1p2*, *Atp1p2k80* and *Atku80* mutants treated with 0, 0.006%, 0.008% or 0.01% MMS. For each treatment 20 seedlings were weighed in triplicate. Fresh weight of the wild-type grown for 2 weeks without MMS was set at 1. Student's test: \*  $P < 0.05$ , \*\*  $P < 0.001$  (comparing mutants with the wild-type of the same treatment).

(□ wild-type (WT); ▨ *Atp1p2*; ■ *Atp1p2k80*; ▤ *Atku80*)

that can be converted into DSBs during replication (20). As discussed previously in chapter 2 and 3, the AtKu80 protein functions mainly in DSBs repair via C-NHEJ, whereas the AtParp proteins play an important role in SSBs repair and probably in B-NHEJ as well.



To quantify the effect of MMS treatment, the fresh weight of seedlings was determined after 2 weeks of continuous MMS treatment (Figure 3). With the highest concentration of MMS (0.01%), all the plant lines were very sick and did not grow at all. With the lower concentrations of MMS (0.006% and 0.008%), the growth of the *Atp1p2* and *Atp1p2k80* mutants was retarded more than the growth of the wild-type and the *Atku80* mutant. In the presence of 0.008% MMS, the fresh weight of the *Atp1p2k80* mutant was reduced to half of the weight of the *Atp1p2* mutant, or one fourth of the weight of the *Atku80* mutant. As expected, the *Atp1p2k80* triple mutant was most sensitive to the exposure of MMS among all the plant lines, probably due to the deficiency of multiple DNA repair pathways in this triple mutant.

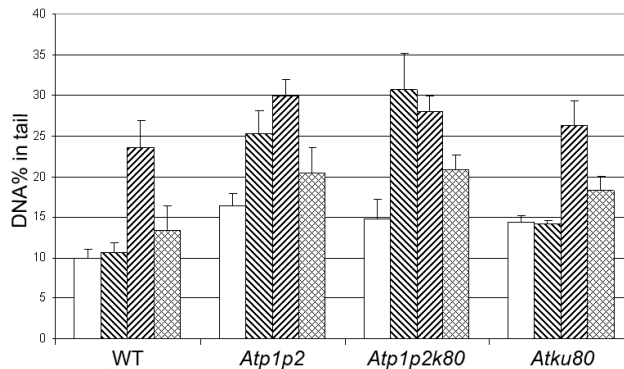


**Figure 4.** Quantification of DNA damage by Comet assay.

The fraction of DNA in comet tails (%tail-DNA) was used as a measure of DNA damage in wild-type plants and *Atp1p2*, *Atp1p2k80* and *Atku80* mutants. Around 100 nuclei for each treatment were analyzed. The means of %tail-DNA after MMS treatment are shown.

(□ t=0; ▨ t=2h; ▩ t=24h; ▤ 24h+24h recovery)

In order to quantify the DNA damage in these mutants after MMS treatment, comet assays (A/N protocol) were performed, that identify SSBs and DSBs. For each treatment, around 100 randomly chosen nuclei from 4 independent mini gel replicas were analyzed by using CometScore™. Without any treatment, the genomic DNA of the *Atp1p2*, *Atp1p2k80* and *Atku80* mutants already had more DNA damage than that of the wild-type, demonstrating that AtParp proteins and AtKu80 are involved in DNA repair systems (Figure 4). The *Atp1p2* and *Atp1p2k80* mutants had a higher level of nuclear DNA damage than the wild-type and the *Atku80* mutant after 2 h MMS treatment, which can be explained by the essential role of the AtParp proteins in SSBs repair. The *Atp1p2k80* triple mutant had more DNA damage than the *Atp1p2* mutant, in accordance with the result of the fresh weight measurements after the MMS treatment. After 24 h MMS treatment, the differences among the various plant lines were not significant, since 24 h MMS treatment was very deleterious to all of them. After 24 h of recovery the DNA damage was repaired in the wild-type to the situation before the treatment. In the mutants about half of the DNA damage was repaired after 24 h recovery compared to the situation before treatment. Since AtKu80 is a major

component of C-NHEJ, DNA repair capacity was expected to be reduced in the *Atku80* mutant. Interestingly, even in the *Atp1p2k80* triple mutant, half of the additional DNA damage was repaired, suggesting the existence of another SSBR pathway besides the AtParp mediated SSBR.

### End joining in the *Atku80*, *Atp1p2* and *Atp1p2k80* mutants

To directly test the function of AtParp proteins and AtKu80 in NHEJ, an *in vivo* plasmid rejoining assay was utilized to quantify the capacity of the *Atparp* and *Atku80* mutants to repair DSBs generated by restriction enzymes. To this end, we transformed protoplasts from leaves with circular (control) or BamHI linearised plasmid DNA. BamHI digests the plasmid DNA in the N-terminal part of the GFP coding sequence. Rejoining of linear plasmid by the NHEJ pathway *in vivo* will result in GFP expression. GFP fluorescence was indeed detected in the wild-type protoplasts which were transformed with the linearized plasmid. But it was difficult to quantify the difference in GFP expression between the wild-type and the mutants under the fluorescence microscope. Therefore, we analyzed the rejoining efficiency by Q-PCR, using primers around the BamHI site compared to primers in the GFP coding region. The results showed that the rejoining efficiency was reduced by half in the *Atku80* mutant compared with the wild-type, whereas the efficiencies were reduced mildly in the *Atp1p2* mutant (Figure 5). This demonstrated that AtKu80, a core component in C-NHEJ, played a crucial role in NHEJ. AtParp proteins could be participants in B-NHEJ. When the C-NHEJ was well functioning, the deficiency in *AtParp* genes did not much influence the capacity of end joining. Surprisingly, the *Atp1p2k80* triple mutant had nearly the same ability of end joining as the wild-type. This suggests that there may be other robust alternative NHEJ pathways in plants, which probably are inhibited by both Ku-dependent C-NHEJ and Parp-dependent B-NHEJ and only become active in the absence of these pathways.

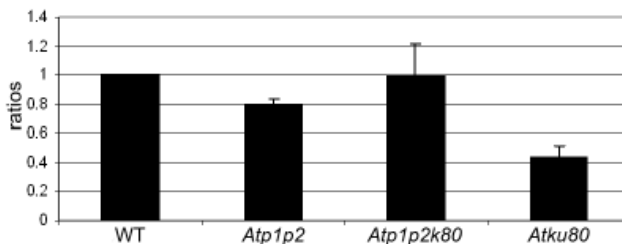


**Figure 5.** Plasmid end joining assay with protoplasts.

Fraction of rejoining plasmid DNA was determined by PCR. The value obtained in wild-type protoplasts was set on 1. Values of end joining in protoplasts from the mutants are given relative to that of the wild-type.

### End joining products of the *Atku80*, *Atp1p2* and *Atp1p2k80* mutants

In order to investigate the mutagenic potential of the different NHEJ pathways, the spectra of end-joining products with DNA substrates with different type of DNA ends was tested with

cell-free protein extracts from leaves of the wild-type and the mutants. Analysis of the joined products showed that the joining was accurate for the DNA substrates with compatible ends of 5'-overhangs, whereas the joining was prone to be inaccurate for the other types of ends, such as compatible 3'-overhangs, incompatible ends and blunt ends (Figure 6). In most cases deletions were produced for inaccurate end joining, suggesting that the DNA substrates

----G GATCC---- ----CCTAG G----	5' overhangs (BamHI)				----TACAGC TGGAA---- ----ATGTCG ACCTTA----	Blunt ends (no homology)			
	WT	<i>Atp1p2</i>	<i>Atp1p2k80</i>	<i>Atku80</i>		WT	<i>Atp1p2</i>	<i>Atp1p2k80</i>	<i>Atku80</i>
BamHI sensitive	13/15	17/17	19/19	14/14	XcmI sensitive	8/15	4/16	1/11	7/19
small deletion<10bp	2/15				small deletion<10bp	5/15	11/16	7/11	9/19
----GGTAC C---- ----C CATGG----	3' overhangs (KpnI)				---TACCATCCTACAGC ATCCTACAGCTGGA--- ---ATGGTAGGATGTCG TAGGATGTCGACCT---	Blunt ends (10bp homology)			
	WT	<i>Atp1p2</i>	<i>Atp1p2k80</i>	<i>Atku80</i>		WT	<i>Atp1p2</i>	<i>Atp1p2k80</i>	<i>Atku80</i>
KpnI sensitive	6/9	7/12	7/11	7/13	joined precisely	7/36	7/23	3/17	2/20
small deletion<10bp	2/9	1/12	2/11	1/13	small deletion<10bp	5/36	10/23	7/17	3/20
large deletion>10bp	1/9			2/13	insertion		3/23	2/17	
insertion		3/12	2/11	3/13	MMEJ (XcmI sensitive)	24/36	3/23	5/17	15/20
substitution		1/12				WT	<i>Atp1p2</i>	<i>Atp1p2k80</i>	<i>Atku80</i>
MMEJ (large deletion)				1/13 (8bp)	Total large deletion (>10bp)	3/76	2/53	5/56	8/67
----GGTAC AATTC---- ----C G----	3' overhang (KpnI) + 5' overhang (EcoRI)								
Filled in	5/16	5/12	2/17	3/15					
small deletion<10bp	11/16	6/12	13/17	9/15					
large deletion>10bp		1/12	2/17	3/15					

**Figure 6.** Plasmid end joining assay with protein extracts.

DNA substrates with compatible 5'-overhangs, compatible 3'-overhangs, incompatible ends, blunt ends without micro-homology and blunt ends with 10 bp micro-homology were used. Spectra of the junctions are shown generated from DNA substrates with different ends in protein extracts from leaves of the wild-type and *Atp1p2*, *Atp1p2k80* or *Atku80* mutants. After end joining, the junction was amplified by PCR and cloned. The number of plasmids with specific types of junctions was shown compared to the total number analyzed.

were prone to be resected. Small deletions (<10 bp) were often seen among the products from all the different plant lines. Large deletions (>10 bp) were rarely obtained for the wild-type and the *Atp1p2* mutant. The number of large deletions, some of which utilized micro-homology, was increased in the *Atku80* and *Atp1p2k80* mutants, suggesting that AtKu80 protected the DNA ends from resection and prevented the formation of deletions. The sequencing results of the different ends are shown in Table 3. The sequencing results of the end joining assay for 5'-overhangs in leaf protoplasts revealed that most of the ends had been joined precisely, except for some small deletions, which occurred in all the different

plant lines. One junction, the result of a large deletion (29-125 bps) on sites of 8 bp micro-homology, was found in the *Atku80* mutant. This also pointed out that AtKu80 may inhibit MMEJ by protecting the DNA ends from resection.

**Table 3.** Sequence results for the in vitro end joining assay.

<b>5' overhangs (BamHI)</b>
CAAGTACCATCCTCAGC <b>G</b> <sup>^</sup> <b>GATCC</b> GAATTCGTAATCATGGTCATAGC
WT
CAAGTACCATCCTCAGC · · <b>ATCC</b> GAATTCGTAATCATGGTCATAGC
CAAGTACCATCCTCAG · · · <b>ATCC</b> GAATTCGTAATCATGGTCATAGC
<b>3' overhangs (KpnI)</b>
CAAGTACCATCCTACAGC <b>GGTAC</b> <sup>^</sup> <b>CGAATTC</b> GTAATCATGGTCATAGC
WT
CAAGTACCATCCTACAGC <b>GGTAC</b> · GAATTCGTAATCATGGTCATAGC (2)
CAAGTACCATCCTACAGC <b>GGT</b> · · -145bp · · · ACTGCCCGCTTCCAGT
<i>Atp1p2</i>
CAAGTACCATCCTACAGC <b>GGTAC</b> · GAATTCGTAATCATGGTCATAGC
CAAGTACCATCCTACAGC <b>GGTAC</b> AGAATTCGTAATCATGGTCATAGC
CAAGTACCATCCTACAGC <b>GGTAC</b> AAC <b>CGAATTC</b> GTAATCATGGTCATAG
CAAGTACCATCCTACAGC <b>GGTAC</b> GTAC <b>CGAATTC</b> GTAATCATGGTCAT (2)
<i>Atp1p2k80</i>
CAAGTACCATCCTACAGC <b>GGTAC</b> · GAATTCGTAATCATGGTCATAGC (2)
CAAGTACCATCCTACAGC <b>GGTAC</b> GTAC <b>CGAATTC</b> GTAATCATGGTCAT (2)
<i>Atku80</i>
CAAGTACCATCCTACAGC <b>GGTAC</b> · GAATTCGTAATCATGGTCATAGC
CAAGTACCATCCTACAGC <b>GGTAC</b> G <b>CGAATTC</b> GTAATCATGGTCATAGC
CAAGTACCATCCTACAGC <b>GGTAC</b> GTAC <b>CGAATTC</b> GTAATCATGGTCAT (2)
AAAATACCGC · · · · · -336bp · · · <b>TACCGAATTC</b> GTAATCATGGTCAT
TCGCTATTACGCCAGCTG · · · · · -291bp · · · · · CATTAAATGAATCGGCCAACCGC
<b>3' overhangs (KpnI) +5' overhangs (EcoRI)</b>
CAAGTACCATCCTACAGC <b>GGTAC</b> <sup>^</sup> <b>C G</b> <sup>^</sup> <b>AATTC</b> GTAATCATGGTCATAGC
CAAGTACCATCCTACAGC <b>GGTACAATTC</b> GTAATCATGGTCATAGC
WT
CAAGTACCATCCTACAGC <b>GGTA</b> · <b>AATTC</b> GTAATCATGGTCATAGC (2)
CAAGTACCATCCTACAGC <b>GGTAC</b> · <b>ATTC</b> GTAATCATGGTCATAGC (3)
CAAGTACCATCCTACAGC <b>GGTA</b> · · <b>ATTC</b> GTAATCATGGTCATAGC
CAAGTACCATCCTACAGC <b>GGTAC</b> · · · <b>TCGTAATCATGGTCATAGC</b>
CAAGTACCATCCTACAGC <b>GGTAC</b> · · · · <b>CGTAATCATGGTCATAGC</b>
CAAGTACCATCCTACAGC <b>GGTAC</b> · · · · · <b>GTAATCATGGTCATAGC</b> (2)
CAAGTACCATCCTACAGC <b>G</b> · · · · · <b>GTAATCATGGTCATAGC</b>
<i>Atp1p2</i>
CAAGTACCATCCTACAGC <b>GGTA</b> · <b>AATTC</b> GTAATCATGGTCATAGC (2)
CAAGTACCATCCTACAGC <b>GGTAC</b> · <b>ATTC</b> GTAATCATGGTCATAGC
CAAGTACCATCCTACAGC <b>GGTAC</b> · · · · · <b>GTAATCATGGTCATAGC</b> (2)
CAAGTACCATCCTACAGC <b>GGTA</b> · · · · · <b>GTAATCATGGTCATAGC</b>
CAAGTACCATCCTACAGC <b>G</b> · · · -75bp · · · <b>GTCACAATTCACACAA</b>

*Atp1p2k80*

CAAGCTACCATCCTACAGC**GGTA**·**AATTC**CGTAATCATGGTCATAGC  
CAAGCTACCATCCTACAGC**GGTAC**·**ATTC**CGTAATCATGGTCATAGC (3)  
CAAGCTACCATCCTACAGC**GGTAC**··**TTC**CGTAATCATGGTCATAGC  
CAAGCTACCATCCTACAGC**GGTAC**···**TCG**TAATCATGGTCATAGC  
CAAGCTACCATCCTACAGC**GGTAC**····**CG**TAATCATGGTCATAGC (3)  
CAAGCTACCATCCTACAGC**GGTAC**·····GTAATCATGGTCATAGC (4)  
CAAGCTACCATCCTACAGC**GGTAC**····-12bp···ATGGTCATAGC  
CAAGCTACCATCCTACAGC**GGTAC**·····-14bp····GGTCATAGC

*Atku80*

CAAGCTACCATCCTACAGC**GGTA**·**AATTC**CGTAATCATGGTCATAGC  
CAAGCTACCATCCTACAGC**GGTAC**·····GTAATCATGGTCATAGC (4)  
CAAGCTACCATCCTACAGC**GGTA**·····GTAATCATGGTCATAGC (3)  
CAAGCTACCATCCTACAGC**GGTA**······AATCATGGTCATAGC  
CAAGCTACCATCCTACAGC**GGTAC**·····-14bp····GGTCATAGC  
CAAGCTACCATCCTACAGC**GGTAC**·····-41bp·····TTATCCGC  
CAAGCTACCATCCTACAGC**GGTAC**·····-118bp·····TAATGAG

**Blunt ends without micro-homology**

GTGCCAAGCTACCATCCTACAGC^TGGAATTCGTAATCATGGTCATAGC

WT

GTGCCAAGCTACCATCCTACA····GAATTCGTAATCATGGTCATAGC  
GTGCCAAGCTACCATCCTAC·····GAATTCGTAATCATGGTCATAGC (2)  
GTGCCAAGCTACCATCCTACAG····AATTCGTAATCATGGTCATAGC  
GTGCCAAGCTACCATCC······GAATTCGTAATCATGGTCATAGC  
GTGCCAAGCTACCATCCTA·····-91bp····AGTGTAAGCCTGGG  
TCAGAGCAGATTG····-251bp···GAATTCGTAATCATGGTCATAGC

*Atp1p2*

GTGCCAAGCTACCATCCTACAG··GGAATTCGTAATCATGGTCATAGC (2)  
GTGCCAAGCTACCATCCTACAG···GAATTCGTAATCATGGTCATAGC  
GTGCCAAGCTACCATCCTACA···GGAATTCGTAATCATGGTCATAGC (4)  
GTGCCAAGCTACCATCCTAC····GGAATTCGTAATCATGGTCATAGC (2)  
GTGCCAAGCTACCATCCTA·····GAATTCGTAATCATGGTCATAGC  
GTGCCAAGCTACCATCCTACA·····ATTTCGTAATCATGGTCATAGC  
GCCAAGCTACC·····-11bp····GGAATTCGTAATCATGGTCATAG

*Atp1p2k80*

GTGCCAAGCTACCATCCTACAG·TGGAATTCGTAATCATGGTCATAGC (1)  
GTGCCAAGCTACCATCCTACAGC··GAATTCGTAATCATGGTCATAGC (2)  
GTGCCAAGCTACCATCCTACAG···GAATTCGTAATCATGGTCATAGC  
GTGCCAAGCTACCATCCTACAG····AATTCGTAATCATGGTCATAGC  
GTGCCAAGCTACCATCCTACA····GAATTCGTAATCATGGTCATAGC (2)  
GTGCCAAGCTACCATCCT·····-24bp·····CATAGC  
GTGCCAAGCTACCATCCTA·····-28bp·····C  
GTGCCAAGCTACCATCCTACAGC····-78bp·····CCGGAAGCAT

<p><i>Atku80</i></p> <p>GTGCCAAGCTACCATCCTACAGC · · GAATTCGTAATCATGGTCATAGC  GTGCCAAGCTACCATCCTACAG · · GGAATTCGTAATCATGGTCATAGC  GTGCCAAGCTACCATCCTACAG · · · GAATTCGTAATCATGGTCATAGC  GTGCCAAGCTACCATCCTACA · · · GGAATTCGTAATCATGGTCATAGC  GTGCCAAGCTACCATCCTAC · · · · GGAATTCGTAATCATGGTCATAGC  GTGCCAAGCTACCATCCTAC · · · · · GAATTCGTAATCATGGTCATAGC (2)  GTGCCAAGCTACCATCCTAC · · · · · AATTCGTAATCATGGTCATAGC  GTGCCAAGCTACCATCC · · · · · GAATTCGTAATCATGGTCATAGC  GCCAAGCTACCATC · · · · · -22bp · · · · · ATGGTCATAGC  CCAGTGCCAAGCTACCATCC · · · -56bp · · · GCTCACAATTCCACACAACA  ACGCCAGGGTTTTCCAGTC · · · -204bp · · · GGGAAACCTGTCGTGCCAG</p>
<p><b>Blunt ends with micro-homology</b></p> <p>GTGCCAAGCTACCATCCTACAGC <u>^ATCCTACAGCTGGAATTCGTAATCA</u>  WT  GTGCCAAGCTACCATCCTACAG · ATCCTACAGCTGGAATTCGTAATCA (5)</p>
<p><i>Atp1p2</i></p> <p>GTGCCAAGCTACCATCCTACAG · ATCCTACAGCTGGAATTCGTAATCA (8)  GTGCCAAGCTACCATCCTA · · · · ATCCTACAGCTGGAATTCGTAATCA (2)  GTGCCAAGCTACCATCCTACAGCAATCCTACAGCTGGAATTCGTAATCA  GTGCCAAGCTACCATCCTACAGCGGATCCTACAGCTGGAATTCGTAATCA  GTGCCAAGCTACCATCCTACAGCGTGATCCTACAGCTGGAATTCGTAATC</p>
<p><i>Atp1p2k80</i></p> <p>GTGCCAAGCTACCATCCTACAG · ATCCTACAGCTGGAATTCGTAATCA (5)  GTGCCAAGCTACCATCCTAC · · · ATCCTACAGCTGGAATTCGTAATCA  GTGCCAAGCTACCATCCTA · · · · ATCCTACAGCTGGAATTCGTAATCA  GTGCCAAGCTACCATCCTACAGCATCCTACAGCTGGAATTCGTAATCA  GTGCCAAGCTACCATCCTACAGCTGGGAATCCTACAGCTGGAATTCGTAA</p>
<p><i>Atku80</i></p> <p>GTGCCAAGCTACCATCCTACAG · ATCCTACAGCTGGAATTCGTAATCA (2)  GTGCCAAGCTACCATCCTA · · · · ATCCTACAGCTGGAATTCGTAATCATG</p>

The recognition sequences for restriction enzymes are shown as bold letters. The number in brackets indicates multiple clones obtained for that sequence. The dots represent the deletion and the italic letters represent the insertion. The micro-homologous sequences are underlined.

In order to test whether AtParp proteins are involved in MMEJ, a DNA substrate with blunt ends containing 10 bp micro-homology sequences was used for end-joining assays in the wild-type and *Atp1p2*, *Atku70*, *Atku80* and *Atp1p2k80* mutants as described for the *Atparp* mutants in chapter 3. When end joining occurs via MMEJ using the 10 bp microhomology, an XcmI site (CCAN9TGG) will be generated (chapter 3). To determine the fraction of the products joined via MMEJ using the 10 bp microhomology, the PCR products were digested with XcmI. Compared with the wild-type, the *Atp1p2* and *Atp1p2k80* mutants had about two fold less MMEJ products, whereas the *Atku* mutants had about two fold more MMEJ products, indicating that the AtParp proteins are involved in MMEJ (chapter 3), while the AtKu proteins prevent MMEJ by the AtParp proteins (Figure 7). This

suggested that there is a competition between AtParp and AtKu proteins to regulate the use of different NHEJ pathways. The products that were not repaired via MMEJ were also sequenced and these turned out to contain small deletion or insertions.

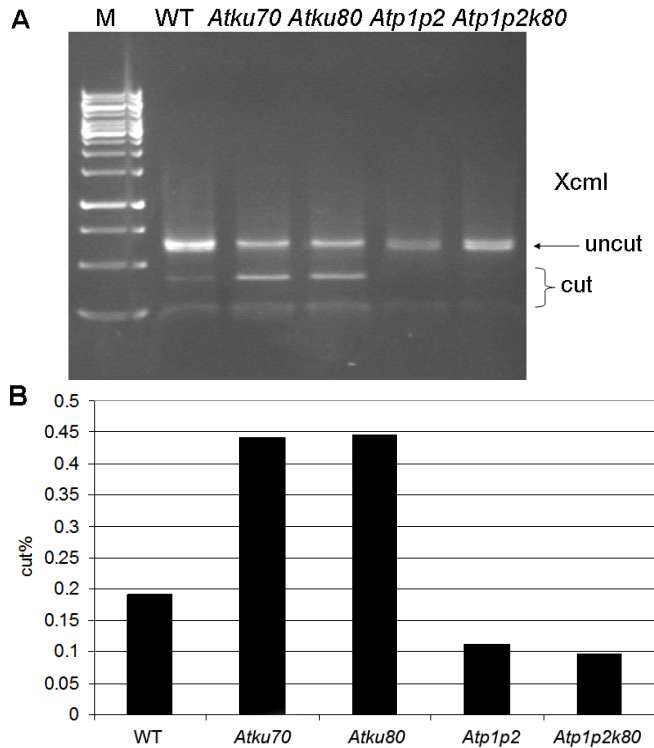


**Figure 7.** MMEJ catalyzed by protein extracts from leaves.

(A) After incubation of linear DNA substrate with protein extracts, a 600-bp fragment was PCR-amplified on the end-joined products and subsequently digested with XcmI. Only the products joined via MMEJ can be digested with XcmI resulting in two fragments of 400 bp and 200 bp. (B) Quantification of MMEJ activity from (A). The relative contribution of the 10-bp MMEJ was calculated as the percentage of the XcmI-digested fragments of total PCR products (sum of the XcmI-digested and undigested fragments).

### T-DNA integration and gene targeting in the *Atku80*, *Atp1p2* and *Atp1p2k80* mutants

Double strand break repair mechanisms are hypothesized to control the integration of *Agrobacterium* T-DNA in plants. In chapter 2, we found that the *Atku* mutations significantly reduced the floral dip transformation frequency as compared to the wild-type, and in chapter 3 that the absence of AtParp proteins did not cause a significant decrease in T-DNA integration frequency via floral dip. To test if T-DNA integration still can happen when both C-NHEJ and B-NHEJ are blocked, the *Atp1p2k80* mutant was transformed by *Agrobacterium* using the floral dip method. The transformation frequency was determined as the number of Hpt-resistant seedlings per total number of plated seeds. The transformation frequencies of the *Atp1p2k80* mutant was significantly reduced compared with the wild-type, and was even lower than that of the *Atku80* mutant (Figure 8). However T-DNA

integration still happened in the triple mutant when both NHEJ pathways were inactivated.

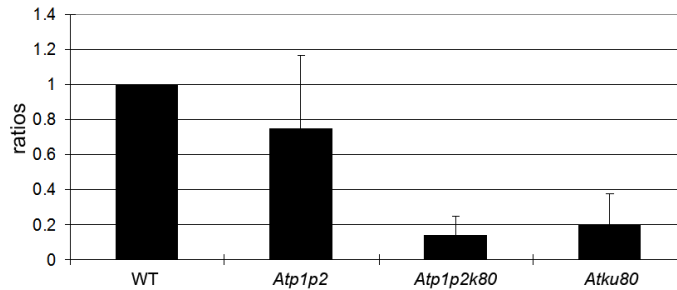


**Figure 8.** Transformation frequencies using the floral dip assay. One gram of seeds from the wild-type and the *Atp1p2*, *Atp1p2ku80* or *Atku80* mutants obtained after floral dip transformations were selected on hygromycin. The number of hygromycin resistant seedlings was scored 2 weeks after germination. The transformation frequency is presented as the ratio of the percentage of hygromycin resistant seedlings in the mutants and the wild-type.

If NHEJ is blocked, the chance for DNA repair via HR could be increased, so that the frequency of gene targeting could also be increased (2;3;21;22). The frequency of gene targeting was tested in the wild-type, the *Atp1p2*, *Atp1p2ku80*, and *Atku80* mutants. About 1 butafenacil-resistant plant in 1000 transformants was found in the wild-type (chapter 2). There were 1 or 2 butafenacil-resistant plants found in around 1000 transformants of the *Atp1p2*, *Atku80* and *Atp1p2ku80* mutants. The butafenacil-resistant plants were analyzed by PCR to determine whether they indeed represented gene targeting events. In case of a GT event, PCR products obtained with the combination of the PPO primers (Figure 2) can be digested by KpnI. The butafenacil-resistant plants of the wild-type were GT events (data not shown). However, the PCR products of the butafenacil-resistant plants of the *Atku80* and *Atp1p2ku80* mutants were resistant to KpnI digestion, indicating they were escapes (data not shown). The butafenacil-resistant plants of the *Atp1p2* mutants were too small for PCR analysis. It seemed that the gene targeting frequency was not significantly increased in the triple mutant compared with the wild-type, suggesting that inactivation of components from both the C-NHEJ and the B-NHEJ pathways did not induce the HR pathway. Together with the results from the T-DNA integration experiments, this indicated that an additional pathway of NHEJ must exist.

## Discussion

Here the *Atp1p2ku80* triple mutant, which was deficient in both Ku-dependent C-NHEJ and Parp-involved B-NHEJ pathways, was obtained and functionally characterized. The triple mutant was more sensitive to the stress of SSBs and DSBs than the wild-type, the *Atp1p2* and *Atku80* mutants, but it could still repair DNA damage to some extent according to the comet assay. The data from end joining assays and floral dip transformations showed that the *Atp1p2ku80* mutant still had ability for end joining and T-DNA integration. All



these results suggested that either there is another alternative NHEJ in plants or that the C-NHEJ and B-NHEJ were not completely inactive in the triple mutant. The end joining capacity of the *Atku80* mutant was much lower than that of the wild-type, while the end joining capacity of the *Atp1p2* mutant was only mildly affected (Figure 5). However, unexpectedly the *Atp1p2k80* triple mutant had a similar end joining capacity as the wild-type. This suggests that indeed an additional pathway is present, which is suppressed under normal conditions, and becomes active when both the C-NHEJ and B-NHEJ are blocked. This hypothesis also explains the residual T-DNA integration and low GT frequency in the triple mutant. Recently, a similar result was also reported from the DNA repair kinetics after  $\gamma$ -irradiation in the *Atku80xcorr1* mutant by Charbonnel et al. (23). Though the *Atp1p2k80* mutant did not reduce the end joining frequency in the leaf protoplasts, it still had lower T-DNA integration frequency via floral dip transformation, compared with the wild-type. Possibly, the additional pathway is less active in the gametophytic cells (used in floral dip transformation) than in the somatic leaf cells (used in the end joining assay). Alternatively, T-DNA integration in chromosomes may be more dependent on C-NHEJ than end joining of naked plasmid molecules.

Results from end joining assays with different DNA ends in cell-free extracts revealed that in the *Atku80* mutant more large deletions were found than in the wild-type, suggesting that Ku80 plays a role in keeping genome integrity in plants. This is in accordance with some reports in mammals, which also showed that Ku may serve as an alignment factor that not only increases NHEJ efficiency but also accuracy (24-28). Though NHEJ is an error-prone DNA repair pathway compared with HR, it still results in a high fidelity when Ku-dependent C-NHEJ is active. Mutation of C-NHEJ core factors resulted in loss of the accuracy of DNA repair (27). As in the results described here, the C-NHEJ deficient mutants preferred end joining using micro-homology so that the chance for deletions was highly increased and the genome was unstable (25;27). Of the known end-joining pathways, C-NHEJ is relatively fast and accurate, so that it is the first choice for the organisms to repair DNA DSBs.

The *Atp1p2* and *Atp1p2k80* mutants gave less MMEJ products than the wild-type, whereas the *Atku80* mutant gave more MMEJ products than the wild-type in the *in vitro* end joining assays (Figure 7). The latter is not consistent with the percentages of the different joined products from the results of sequencing (Figure 6). Sequencing indicated that the *Atku80* mutant formed a similar percentage of MMEJ products as the wild-type. It is possible that the PCR products in Figure 7 were not completely digested. But both experiments indicated that AtParp1 and AtParp2 are involved in MMEJ (chapter 3) and AtKu80 can inhibit MMEJ. These results point to a regulatory mechanism, in which competition between Parp and Ku determines whether C-NHEJ or B-NHEJ is used, as was found for mammalian systems (6). When the Ku protein is absent, Parp may bind the DNA ends and direct the DNA repair pathway to B-NHEJ, which more often uses micro-homology. Katsura *et al.* (29) reported that Ku80 could also be involved in MMEJ, but

MMEJ is less dependent on Ku80 than NHEJ. Recently, it was shown that Ku regulated the choice of repair pathway by inhibition of end processing and thus by repression on HR and MMEJ (30;31). MMEJ leads to deletion and is therefore mutagenic and may be harmful for the genome stability. When the major DNA DSB repair pathway, C-NHEJ, is available, MMEJ is suppressed by C-NHEJ for optimal genome stability. Ku and Parp proteins could be involved in regulating this. The *Atp1p2k80* triple mutant might be used as a tool to further investigate the mechanism of the regulation and to identify components of the additional NHEJ pathways in future.

### Reference List

1. van Attikum,H., Bundock,P. and Hooykaas,P.J. (2001) Non-homologous end-joining proteins are required for *Agrobacterium* T-DNA integration. *EMBO J.*, **20**, 6550-6558.
2. van Attikum,H. and Hooykaas,P.J. (2003) Genetic requirements for the targeted integration of *Agrobacterium* T-DNA in *Saccharomyces cerevisiae*. *Nucleic Acids Res.*, **31**, 826-832.
3. Kooistra,R., Hooykaas,P.J. and Steensma,H.Y. (2004) Efficient gene targeting in *Kluyveromyces lactis*. *Yeast*, **21**, 781-792.
4. Wang,H., Perrault,A.R., Takeda,Y., Qin,W., Wang,H. and Iliakis,G. (2003) Biochemical evidence for Ku-independent backup pathways of NHEJ. *Nucleic Acids Res.*, **31**, 5377-5388.
5. Audebert,M., Salles,B. and Calsou,P. (2004) Involvement of poly(ADP-ribose) polymerase-1 and XRCC1/DNA ligase III in an alternative route for DNA double-strand breaks rejoining. *J. Biol. Chem.*, **279**, 55117-55126.
6. Wang,M., Wu,W., Wu,W., Rosidi,B., Zhang,L., Wang,H. and Iliakis,G. (2006) PARP-1 and Ku compete for repair of DNA double strand breaks by distinct NHEJ pathways. *Nucleic Acids Res.*, **34**, 6170-6182.
7. Alonso,J.M., Stepanova,A.N., Leisse,T.J., Kim,C.J., Chen,H., Shinn,P., Stevenson,D.K., Zimmerman,J., Barajas,P., Cheuk,R. *et al.* (2003) Genome-wide insertional mutagenesis of *Arabidopsis thaliana*. *Science*, **301**, 653-657.
8. Weijers,D., Franke-van Dijk,M., Vencken,R.J., Quint,A., Hooykaas,P. and Offringa,R. (2001) An Arabidopsis Minute-like phenotype caused by a semi-dominant mutation in a RIBOSOMAL PROTEIN S5 gene. *Development*, **128**, 4289-4299.
9. Murashige,T. and Skoog,F. (1962) A Revised Medium for Rapid Growth and Bio Assays with Tobacco Tissue Cultures. *Physiologia Plantarum*, **15**, 473-497.
10. Kozak,J., West,C.E., White,C., da Costa-Nunes,J.A. and Angelis,K.J. (2009) Rapid repair of DNA double strand breaks in *Arabidopsis thaliana* is dependent on proteins involved in chromosome structure maintenance. *DNA Repair (Amst)*, **8**, 413-419.
11. Wang,S., Tiwari,S.B., Hagen,G. and Guilfoyle,T.J. (2005) AUXIN RESPONSE FACTOR7 restores the expression of auxin-responsive genes in mutant Arabidopsis leaf mesophyll protoplasts. *Plant Cell*, **17**, 1979-1993.
12. Liang,L., Deng,L., Nguyen,S.C., Zhao,X., Maulion,C.D., Shao,C. and Tischfield,J.A. (2008) Human DNA ligases I and III, but not ligase IV, are required for microhomology-mediated end joining of DNA double-strand breaks. *Nucleic Acids Res.*, **36**, 3297-3310.
13. Liang,L., Deng,L., Chen,Y., Li,G.C., Shao,C. and Tischfield,J.A. (2005) Modulation of DNA end joining by nuclear proteins. *J. Biol. Chem.*, **280**, 31442-31449.
14. Clough,S.J. and Bent,A.F. (1998) Floral dip: a simplified method for *Agrobacterium*-mediated transformation of *Arabidopsis thaliana*. *Plant J.*, **16**, 735-743.
15. de Pater,S., Neuteboom,L.W., Pinas,J.E., Hooykaas,P.J. and van der Zaal,B.J. (2009)

- ZFN-induced mutagenesis and gene-targeting in Arabidopsis through *Agrobacterium*-mediated floral dip transformation. *Plant Biotechnol. J.*, **7**, 821-835.
16. Masson, J. and Paszkowski, J. (1992) The Culture Response of *Arabidopsis-Thaliana* Protoplasts Is Determined by the Growth-Conditions of Donor Plants. *Plant Journal*, **2**, 829-833.
  17. van Attikum, H., Bundock, P., Overmeer, R.M., Lee, L.Y., Gelvin, S.B. and Hooykaas, P.J. (2003) The Arabidopsis AtLIG4 gene is required for the repair of DNA damage, but not for the integration of *Agrobacterium* T-DNA. *Nucleic Acids Res.*, **31**, 4247-4255.
  18. Hanin, M., Volrath, S., Bogucki, A., Briker, M., Ward, E. and Paszkowski, J. (2001) Gene targeting in Arabidopsis. *Plant J.*, **28**, 671-677.
  19. Burger, R.M., Peisach, J. and Horwitz, S.B. (1981) Activated bleomycin. A transient complex of drug, iron, and oxygen that degrades DNA. *J. Biol. Chem.*, **256**, 11636-11644.
  20. O'Connor, P.J. (1981) Interaction of chemical carcinogens with macromolecules. *J. Cancer Res. Clin. Oncol.*, **99**, 167-186.
  21. Abdel-Banat, B.M., Nonklang, S., Hoshida, H. and Akada, R. (2010) Random and targeted gene integrations through the control of non-homologous end joining in the yeast *Kluyveromyces marxianus*. *Yeast*, **27**, 29-39.
  22. Krappmann, S., Sasse, C. and Braus, G.H. (2006) Gene targeting in *Aspergillus fumigatus* by homologous recombination is facilitated in a nonhomologous end-joining-deficient genetic background. *Eukaryot. Cell*, **5**, 212-215.
  23. Charbonnel, C., Gallego, M.E. and White, C.I. (2010) Xrcc1-dependent and Ku-dependent DNA double-strand break repair kinetics in Arabidopsis plants. *Plant J.*, **64**, 280-290.
  24. Feldmann, E., Schmiemann, V., Goedecke, W., Reichenberger, S. and Pfeiffer, P. (2000) DNA double-strand break repair in cell-free extracts from Ku80-deficient cells: implications for Ku serving as an alignment factor in non-homologous DNA end joining. *Nucleic Acids Res.*, **28**, 2585-2596.
  25. Verkaik, N.S., Esveldt-van Lange, R.E., van Heemst, D., Bruggenwirth, H.T., Hoeijmakers, J.H., Zdzienicka, M.Z. and van Gent, D.C. (2002) Different types of V(D)J recombination and end-joining defects in DNA double-strand break repair mutant mammalian cells. *Eur. J. Immunol.*, **32**, 701-709.
  26. Chen, S., Inamdar, K.V., Pfeiffer, P., Feldmann, E., Hannah, M.F., Yu, Y., Lee, J.W., Zhou, T., Lees-Miller, S.P. and Povirk, L.F. (2001) Accurate in vitro end joining of a DNA double strand break with partially cohesive 3'-overhangs and 3'-phosphoglycolate termini: effect of Ku on repair fidelity. *J. Biol. Chem.*, **276**, 24323-24330.
  27. Kuhfittig-Kulle, S., Feldmann, E., Odersky, A., Kuliczowska, A., Goedecke, W., Eggert, A. and Pfeiffer, P. (2007) The mutagenic potential of non-homologous end joining in the absence of the NHEJ core factors Ku70/80, DNA-PKcs and XRCC4-LigIV. *Mutagenesis*, **22**, 217-233.
  28. Osakabe, K., Osakabe, Y. and Toki, S. (2010) Site-directed mutagenesis in Arabidopsis using custom-designed zinc finger nucleases. *Proc. Natl. Acad. Sci. U. S. A.*, **107**, 12034-12039.
  29. Katsura, Y., Sasaki, S., Sato, M., Yamaoka, K., Suzukawa, K., Nagasawa, T., Yokota, J. and Kohno, T. (2007) Involvement of Ku80 in microhomology-mediated end joining for DNA double-strand breaks in vivo. *DNA Repair (Amst)*, **6**, 639-648.
  30. Fattah, F., Lee, E.H., Weisensel, N., Wang, Y., Lichter, N. and Hendrickson, E.A. (2010) Ku regulates the non-homologous end joining pathway choice of DNA double-strand break repair in human somatic cells. *PLoS. Genet.*, **6**, e1000855.
  31. Roberts, S.A., Strande, N., Burkhalter, M.D., Strom, C., Havener, J.M., Hasty, P. and Ramsden, D.A. (2010) Ku is a 5'-dRP/AP lyase that excises nucleotide damage near broken ends. *Nature*, **464**, 1214-1217.